Ultrathin Mn films on Cu(111) substrates: Frustrated antiferromagnetic order

D. Spišák and J. Hafner
Institut für Materialphysik and Center for Computational Materials Science, Universität Wien, Sensengasse 8/12, A-1090 Wien, Austria
(Received 1 December 1999)

Using local-spin density calculations performed in the generalized-gradient approximation we have examined the possibility that Mn monolayers epitaxially grown on Cu(111) substrates represent a physical realization of the frustrated antiferromagnetic planar (AFP) model. Indeed, we find that the noncollinear ground state of the AFP model with $\pm 120°$ orientations of the nearest-neighbors is also the ground state of Mn/Cu(111). However, due to the rather long-range antiferromagnetic interactions, the energetic preference over a raw-wise antiferromagnetic order is only very weak.

Frustrated two-dimensional spin systems display a very rich phase diagram and critical phenomena. One of the simplest examples of such frustrated systems is the antiferromagnetic planar (or XY) model on a triangular lattice.[1] The antiferromagnetic planar (AFP) model is specified by the model Hamiltonian

$$H = -\sum_{\langle ij \rangle} J_{ij} \vec{S}_i \vec{S}_j = -\sum_{\langle ij \rangle} J_{ij} \cos(\theta_i - \theta_j), \qquad (1)$$

where θ_i is the angle of the planar spin at site i with respect to some reference axis within the plane. The ground state of this Hamiltonian on a triangular lattice has $(\sqrt{3}\times\sqrt{3})$ periodicity and consists of three interpenetrating sublattices with spins on different sublattices forming angles $\pm 120°$ [see Fig. 1(c)]. The noncollinear ground state is degenerate: there exist two topologically distinct classes of the pattern shown in Fig. 1(c) characterized by different helicities. To each triangle a helicity defined as $\Sigma_{\triangle} \Delta\theta/2\pi$ is assigned, where $\Delta\theta$ is the smallest clockwise change in the orientation of the spins when the three vertices are traversed in clockwise direction. In the ground state of the AFP model every triangle has helicity $+1$ or -1 and is surrounded only by triangles of opposite helicity. In the two degenerate ground states, the helicity patterns are exactly out of phase.

An interesting physical realization of the AFP model could consist of antiferromagnetic monolayers grown on the hexagonal (0001) surfaces of hcp or (111) surfaces of fcc crystals which are nonmagnetic or ferromagnetic. The epitaxial growth of ultrathin Mn films on the (111) surfaces of fcc Pd,[2] Ir,[3] Cu,[4–6] and MgO,[7] and on the (0001) surface of Ru (Ref. 8) and Co (Ref. 9) has been studied by various experimental techniques. Deposited on these surfaces, Mn first assumes a close-packed structure with a lattice parameter close to that of fcc Mn. When the layer exceeds a critical thickness, which ranges between 2 and 12 Å, the film undergoes a $(\sqrt{3}\times\sqrt{3})$ reconstruction and the new structure is called the ''expanded'' phase. The expanded phase has been described as a monoatomic Laves-phase ($MgCu_2$-type) (Ref. 8) or as trigonally distorted α-Mn.[6] Here we are interested mainly in the magnetic properties of the ultrathin strained γ-Mn films. The magnetic properties of the overlayers are of evident importance for the stabilization of thin-film growth: The lattice constant of γ-Mn extrapolated from temperatures above 1370 K is $a = 3.73$ Å, leading to a misfit of $+4.3\%$ to Pd ($a_{Pd} = 3.89$ Å) and a misfit of -3.2% to Cu ($a_{Cu} = 3.61$ Å). Spin-polarized total energy calculations performed in the local-spin-density approximation (LSDA) with generalized gradient corrections (GGC) have demonstrated that magnetism leads to a strong expansion of both the energetically unfavorable ferromagnetic ($a^{FM} = 3.87$ Å) and the stable antiferromagnetic high-spin phases ($a^{AFM} = 3.65$ Å) compared to nonmagnetic γ-Mn($a^{NM} = 3.51$ Å),[10,11] suggesting that AFM γ-Mn matches very well with fcc-Cu ($a_{Cu} = 3.64$ Å as calculated in the LSDA + GGC). However, one has to remember that the reduced dimensionality in a monolayer can lead to an enhanced magnetism and hence, due to magnetovolume expansion, to an increased misfit. This is precisely what happens for Mn-monolayers: In a hexagonal AFM Mn-monolayers, the magnetic moment increases to $m = 3.61$ μ_B (compared to 2.4 μ_B in bulk γ-Mn) and the in-plane interatomic distance to $d = 2.62$ Å [compared to $d_{Mn} = 2.58$ Å and $d_{Cu} = 2.57$ Å in the (111) planes of γ-Mn and fcc Cu, respectively]. Hence the conditions for epitaxial growth remain favorable. Detailed studies of ultrathin Mn/Cu(100) films[11–13] have demonstrated that the high-spin antiferromagnetism of homogeneous Mn overlayers plays a crucial role in determining the structure and stability of the films. However it has also been demonstrated that films grown above a certain critical deposition temperature tend to form CuMn surface alloys and to assume a ferromagnetic ground state (with even larger magnetostructural effects).

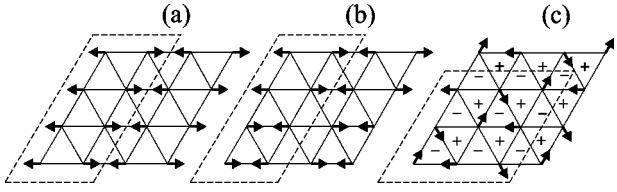

FIG. 1. Collinear (a), and (b) and noncollinear (c) spin-configurations considered for hexagonal Mn overlayers on Cu(111). Configuration (c) corresponds to the ground state of the antiferromagnetic planar (XY) model with the helicity pattern represented by + and − signs. The dashed lines circumscribe the (4×2) and (3×3) surface cells.

TABLE I. Total energies differences and magnetic moments for Mn/Cu(111) films.

Configuration	ΔE (meV/atom)	Site	m_x (μ_B)	m_y (μ_B)	$\lvert m\rvert$ (μ_B)
Noncollinear (c)	0.0	Mn1	1.66	2.87	3.31
		Mn2	1.66	−2.87	3.31
		Mn3	−3.31	0.00	3.31
		Mn4	−3.32	0.00	3.32
		Mn5	1.66	2.87	3.31
		Mn6	1.65	−2.87	3.31
		Mn7	1.66	−2.87	3.32
		Mn8	−3.32	0.00	3.32
		Mn9	1.66	2.87	3.31
Collinear (a)	1.9	Mn1	3.19	0.00	3.19
		Mn2	−3.19	0.00	3.19
Collinear (b)	110.6	Mn1	3.22	0.00	3.22
		Mn2	−3.22	0.00	3.22

Very little is known about magnetic properties of Mn films grown on (111) substrates. Mn/Pd(111) are ''believed'' to be magnetic, most probably antiferromagnetic.[2,4] For Mn/Cu(111), the ''expanded'' structure formed beyond a critical thickness is described as antiferromagnetic with a transition temperature close to 2 K,[5,6] but nothing is known about the magnetic properties in the monolayer limit.

In this paper we use a first-principle local-spin-density approach to calculate the magnetic and electronic structure of Mn monolayers with an epitaxial relationship to the Cu(111) substrate. To deal with the frustration, which is inevitably present in the overlayer, a noncollinear magnetic ordering is allowed. Our calculations have been performed using the noncollinear spin-polarized real-space tight-binding linear muffin-tin orbital (RS-TB-LMTO) technique developed in our group.[14,15] Exchange and correlation have been described by the local-spin-density functional of Ceperley and Alder[16] as parametrized by Perdew and Zunger,[17] adding generalized gradient corrections in the form proposed by Perdew and Wang.[18] The use of gradient corrections is essential because the LSDA leads to an incorrect description of the magnetic ground state of Mn, while gradient corrected functional leads to full agreement with experiment. The LSDA yields an almost complete degeneracy of FM, AFM and NM configurations of fcc, bcc and hcp Mn, whereas GGC's lift the degeneracy and predict the correct moment and volume for the high-spin state of fcc Mn. Likewise, it has been demonstrated that GGC's have a pronounced influence on the magnetism, interatomic distance and magnetic and structural energies of square and hexagonal Mn monolayers.[10,11] For technical details relating to the handling of noncollinearity, we refer to our earlier publications. Here we emphasize only that the stability of noncollinear configurations may be verified by checking that transverse components of the moments relative to the local axis of quantization vanish. Our calculations have been performed for slabs containing 14 layers of Cu, one layer of Mn and three layers of empty spheres allowing for the relaxation of the charge- and spin-densities at the free surface. The potential parameters of the lowest 11 Cu-layers have been held fixed at their bulk values. The models are periodically repeated in the lateral directions so that the clusters on which the real-space recursion has been performed contain up to about 1150 atoms. Along the direction normal to the surface the free boundary conditions were applied. 10, 15, and 45 recursion steps have been used for *s*, *p*, and *d* orbitals.

TABLE II. Exchange coupling constants J_{ij} (meV) calculated for the two frustrated AFM configurations of Mn/Cu(111). The sign of J_{ij} has been chosen such that negative values indicate frustrated interactions, cf. text.

Configuration	Neighbor	Type of coupling	Number of neighbors	J_{ij} (meV)
Collinear (a)	1st	↑↑	2	−35.5
		↑↓	4	56.5
	2nd	↑↑	2	−19.7
		↑↓	4	10.9
	3rd	↑↑[a]	2	−16.0
		↑↑[b]	4	−14.0
Collinear (b)	1st	↑↑	2	−40.1
		↑↓	4	43.9
	2nd	↑↑	2	−26.9
		↑↓	4	1.8
	3rd	↑↑	2	−15.6
		↑↓	4	13.2

[a]Along $\vec{x}$ direction.

[b]Along $\vec{y}$ and $(\vec{x}-\vec{y})$ directions.

In our calculations we have considered two possible collinear AFM and one noncollinear configurations, see Fig. 1. In any collinear AFM configuration, one third of nearest-neighbor interactions is necessarily frustrated, the two configurations shown in Figs. 1(a) and 1(b) differ by the arrangement of the frustrated bounds on straight and zig-zag lines, respectively. The noncollinear configuration shown in Fig. 1(c) corresponds just to the ground state of the AFP model. The (4×2) surface cells with eight atoms treated as inequivalent atoms for the collinear configurations have been chosen such as to contain approximately the same number of atoms as the (3×3) cell with nine atoms of the ground state of the AFP model so that the total energies may be safely compared. The results compiled in Table I demonstrate that the noncollinear configuration is energetically slightly more favorable that the collinear configuration (a) with straight lines of frustrated bonds, whereas the collinear configuration (b) is energetically strongly disfavored. The Mn atoms assume a high-spin state with absolute values of the magnetic moments of $3.2\mu_B$ to $3.3\mu_B$ (the higher moment referring to the noncollinear configuration). These magnetic moments are only slightly lower than in the free standing hexagonal collinear AFM monolayer, $|m|=3.6\mu_B$, but quite generally the moments in hexagonal Mn layers are lower than in square Mn monolayers, $|m|=3.75\mu_B$.[11] The difference between the two collinear configurations may be easily understood by analyzing the exchange coupling constants J_{ij} calculated by the torque-force approach described in our earlier work.[19] For the two collinear configurations the exchange parameters

are listed in Table II. The sign of J_{ij} is chosen such that for a given relative orientation of a pair of spins $J_{ij}>0$ reflects a stabilizing and $J_{ij}<0$ a destabilizing (frustrated) interaction [note that this convention for the sign of J_{ij} differs from that adopted in Eq.(1)]. All interactions up to the third neighbors at twice the nearest-neighbor distance are antiferromagnetic. The decisive difference in favor of configuration (a) comes from the second-neighbor coupling where in configuration (b) we find four strong destabilizing FM and only two very weak stabilizing AFM interactions, whereas in configuration (a) we have four stabilizing AFM and only two destabilizing FM couplings of comparable strength.

The energy difference between the collinear configuration and the noncollinear configuration (a) corresponding to the ground state of the AFP model is surprisingly small—taking the numerical uncertainty into account the two configurations must be considered as practically degenerate. The reason for the very weak preference for the noncollinear structure has to be attributed to beyond-nearest neighbor interactions. In fact for the AFP ground state all six second-neighbor pairs show FM alignment, and only third nearest neighbors show 120° orientations characteristic for nearest-neighbor spins in the AFP model. Although the exchange-pair interactions are configuration-dependent (and cannot, for the moment, be calculated for the noncollinear configuration), our results listed in Table II provide sufficient evidence for the rather long-ranged nature of the exchange interaction in Mn/Cu(111) films and for preferentially AFM second-neighbor coupling.

Finally we analyze very briefly the electronic structure of the Mn overlayers. Figure 2 shows the spin-resolved electronic density of states (DOS) on the Mn sites, for the noncollinear configuration spin up/down refers to the local axis of quantization. All configurations are characterized by a large exchange splitting, the ratio of the local magnetic moment and the exchange splitting (measured in terms of the center of gravity of the *d*-bands) leads to an effective Stoner parameter of $I=0.955\pm0.004$ eV μ_B^{-1} indicating the itinerant character of the magnetism in this system. A remarkable feature is that the minority DOS of the noncollinear configuration shows a very sharp structure, with a DOS peak pinned at the Fermi level. One should also note the similarity of the electronic DOS of the energetically degenerate configurations (a) and (c) (noncollinear).

During completion of this manuscript, we became aware of the recent work of Asada *et al.*,[20] reporting LSDA calculations for free-standing triangular Mn monolayers and Mn/Cu(111) films. In contrast to our results, a row-wise antiferromagnetic collinear configuration was claimed to be energetically more favorable than $(\sqrt{3}\times\sqrt{3})$ noncollinear configuration. Even more surprisingly, the noncollinear configuration with $\pm120°$ orientatons of the nearest-neighbor spins was reported to be unstable against a further increasing of the rotation angle of the spins in the $(\sqrt{3}\times\sqrt{3})$ cell, resulting in a ferrimagnetic structure with hexagonal symmetry (the majority collinear moments are arranged on a honeycomb lattice, moments at the center of the hexagons pointing into opposite directions so that a net total magnetization develops). In addition the moments are substantially smaller than in the free-monolayer calculations of Eder *et al.*,[11] and found in the present work on Mn/Cu(111). The discrepancy between the present results and those of Asada *et al.*[20] is clearly due to their neglect of gradient corrections which minimizes the energy differences between the antiferromagnetic and ferrimagnetic configurations.

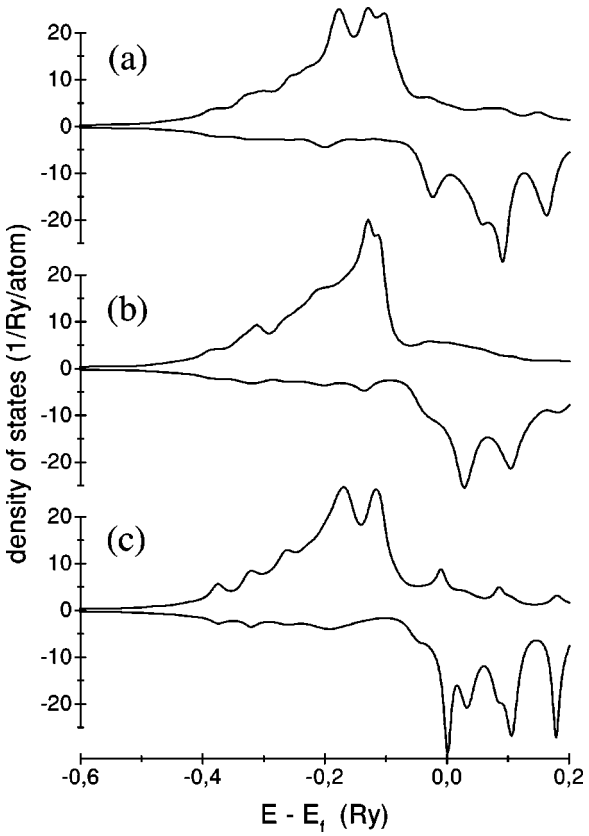

FIG. 2. Spin-resolved electronic densities of states for the three magnetic configurations of Mn/Cu(111). Cf. Fig. 1. For the noncollinear configuration majority/minority densities of states are defined relative to the local spin quantization axis.

To summarize, we have examined the possibility that Mn overlayers grown on Cu(111) substrates represent a physical realization of the AFP model. Indeed we find that the ground state of the AFP model is also the most energetically favorable magnetic configuration for the hexagonal Mn monolayers. However, the energetic preference over a collinear state minimizing the frustrations between second-neighbor spins is only minimal, because the antiferromagnetic second-neighbor coupling (neglected in the AFP model) disfavors the noncollinear $\pm120°$ spin orientations.

This work has been supported by the Austrian Ministry for Science and Transport within the project ''Magnetism on the Nanometer Scale'' and through the Center for Computational Materials Science. The work was part of the network Training and Mobility of Researchers (TMR) program ''Electronic Structure Calculations of Materials Properties and Processes for Industry and Basic Science'' sponsored by the European Union.

[1] D.H. Lee, J.D. Joannopoulos, J.W. Negele, and D.P. Landau, Phys. Rev. B **33**, 450 (1986).
[2] D. Tian, H. Li, S.C. Wu, F. Jona, and P.M. Marcus, Phys. Rev. B **45**, 3749 (1992).
[3] S. Andrieu, H.M. Fischer, M. Piecuch, A. Traverse, and J. Mimault, Phys. Rev. B **54**, 2822 (1996).
[4] D. Tian, A.M. Begley, and F. Jona, Surf. Sci. Lett. **273**, L393 (1992).
[5] I.L. Grigorov and J.C. Walker, J. Appl. Phys. **81**, 3907 (1997).
[6] I.L. Grigorov, J.C. Walker, M.E. Hawley, G.W. Brown, M. Lütt, and M.R. Fitzsimmons, J. Appl. Phys. **83**, 7010 (1998).
[7] I.L. Grigorov, M.R. Fitzsimmons, I-Liang Siu, and J.C. Walker, Phys. Rev. Lett. **82**, 5309 (1999).
[8] A.S. Arrott, B. Heinrich, S.T. Purcell, J.F. Cochran, and L.B. Urquhart, J. Appl. Phys. **61**, 3721 (1987).
[9] K. Ounadjela, P. Vennegues, Y. Henry, A. Michel, V. Pierron-Bohnes, and J. Arabski, Phys. Rev. B **49**, 8561 (1994).
[10] T. Asada and K. Terakura, Phys. Rev. B **47**, 15 992 (1993).
[11] M. Eder, J. Hafner, and E.G. Moroni, Phys. Rev. B (to be published).
[12] O. Rader, W. Gudat, C. Carbone, E. Vescovo, S. Blügel, R. Kläsges, W. Eberhardt, M. Wuttig, J. Redinger, and F.J. Himpsel, Phys. Rev. B **55**, 5404 (1997).
[13] T. Flores, M. Hansen, and M. Wuttig, Surf. Sci. **279**, 251 (1992).
[14] R. Lorenz and J. Hafner, J. Magn. Magn. Mater. **139**, 209 (1995).
[15] D. Spišák and J. Hafner, Phys. Rev. B **55**, 8304 (1997).
[16] D.M. Ceperley and B.J. Alder, Phys. Rev. Lett. **45**, 566 (1980).
[17] J. Perdew and A. Zunger, Phys. Rev. B **23**, 5048 (1981).
[18] J.P. Perdew and Y. Wang, Phys. Rev. B **45**, 13 244 (1992).
[19] D. Spišák and J. Hafner, J. Magn. Magn. Mater. **166**, 303 (1997).
[20] T. Asada, G. Bihlmayer, S. Handschuh, S. Heinze, Ph. Kurz, and S. Blügel, J. Phys.: Condens. Matter **11**, 9347 (1999).